Rec'd JUL 1 1946

FILE COPY
No. 1

NATIONAL ADVISORY COMMITTEE FOR AERONAUTICS

TECHNICAL NOTE

No. 1084

THE EFFECT OF SIMULATED ICING ON PROPELLER PERFORMANCE

By Blake W. Corson, Jr. and Julian D. Maynard

Langley Memorial Aeronautical Laboratory
Langley Field, Va.

Washington
June 1946

FILE COPY
To be Returned to the Files of
Ames Aeronautical Laboratory
National Advisory Committee
for Aeronautics
Moffett Field, Calif.

NATIONAL ADVISORY COMMITTEE FOR AERONAUTICS

TECHNICAL NOTE NO. 1084

THE EFFECT OF SIMULATED ICING ON PROPELLER PERFORMANCE

By Blake W. Corson, Jr. and Julian D. Maynard

SUMMARY

Tests of a 10-foot-diameter three-blade Curtiss 89301-15 propeller with Clark Y blade sections have been conducted in the Langley 16-foot high-speed tunnel in order to determine the effect of simulated ice on the aerodynamic characteristics of the propeller. An irregular coat of cement and fabric was used on the blades to simulate in outline and thickness a formation of glaze ice that might be formed in flight. The propellers were tested on a new 2000-horsepower dynamometer, a brief description of which is included. All tests were made at a rotational speed of 1800 rpm for blade angles of 20°, 25°, 30°, 35°, and 40° at the 42-inch radius and at airspeeds varying from 120 to 420 miles per hour. The results are representative of full-scale constant-speed propeller operation.

The simulated icing condition caused a decrease in peak efficiency of 2.5 to 3.0 percent; this decrease was a result of a loss of blade section lift and increase of blade section drag.

The characteristics of a propeller similar to the one tested were calculated from airfoil data obtained on a wing with and without simulated ice. The calculations indicate a probable loss of peak efficiency of 5.0 percent, which is in fair agreement with the test results. Inasmuch as operation of the entire airplane is affected adversely by ice formation, the airplane when iced may be forced to attempt to climb at relatively low speed and at a high value of thrust coefficient. For this condition the calculations indicate that the propeller efficiency may be about 15 percent less than for an un-iced propeller.

INTRODUCTION

Ice accumulation on aircraft propellers has received considerable attention in recent years as evidenced by the numerous anti-icing devices developed commercially. Prevention of ice deposits on propeller blades in flight is believed to be desirable for two reasons: first, to avoid unbalance of the propeller due to the uneven distribution of the ice and, second, to prevent a loss of aerodynamic efficiency. Previous tests on a wing (reference 1) indicate an increase in section drag and a decrease in section lift of an airfoil with a simulated ice formation; consequently, the least aerodynamic effect that may be expected from ice formation on a propeller is a loss of efficiency due to the decreased lift-drag ratio of the blade sections.

The purpose in making the present tests was to determine the effect of the simulated ice on the aerodynamic characteristics of the propeller throughout a range of advance ratio representative of full-scale constant-speed propeller operation. The tests were made in the Langley 16-foot high-speed tunnel. Photographs of iced propeller blades have been made during flight tests to determine typical ice formations. The irregular coat of cement and fabric used on the propeller tested is believed to simulate a frequently observed and probably mild formation of glaze ice. A more severe ice formation is quite possible, inasmuch as pilots have reported experiences in which the use of full rated power of the engines would not maintain level flight, although the wings and empennage of the airplane were relatively free of ice.

SYMBOLS

M	air-stream Mach number
V	airspeed, feet per second
V_d	wind-tunnel datum velocity, feet per second
n	propeller rotational speed, rps
D	propeller diameter, feet

J propeller advance ratio (V/nD)

J_d nominal propeller advance ratio based on tunnel datum velocity

ρ mass density of air, slugs per cubic foot

P power absorbed by the propeller, foot-pounds per second

T propeller thrust, pounds

C_T thrust coefficient $(T/\rho n^2 D^4)$

C_P power coefficient $(P/\rho n^3 D^5)$

η propeller efficiency $\left(\frac{C_T J}{C_P}\right)$

μ Glauert's velocity correction for wind-tunnel wall interference $(V = \mu V_d;\ J = \mu J_d)$

x fraction of tip radius (r/R)

R radius to tip, feet

r radius to a station, feet

β blade angle, degrees

h blade section maximum thickness, feet

b blade chord, feet

α angle of attack, degrees

APPARATUS

NACA 2000-Horsepower Propeller Dynamometer

The 2000-horsepower propeller dynamometer used in testing the propellers is a new machine still in the development stage. Photographs of the dynamometer in the configuration used for the present tests are shown in figures 1 and 2. The dynamometer is powered by two

1000-horsepower electric motors arranged in tandem. The rated speed is 2100 rpm with a permissible overspeed of 2280 rpm. An accurately controllable variable-frequency power supply provides independent speed control for each motor with rotation in either direction. For dual rotation each motor drives one propeller of the dual unit, and the characteristics of each propeller may be determined independently of the other. For single rotation the motors can be coupled and the power of both motors can be expended through the single propeller.

The dynamometer consists of a heavy steel housing and a support strut, which enclose the motors, thrust capsules, and auxiliary equipment. The support strut is bolted rigidly to the floor of the wind tunnel and streamline tension struts extending from the tunnel walls on each side support the dynamometer laterally.

The motors are supported in the housing in such a way that their casings are free to rotate and also free to move axially with their shafts. Torque is measured by a pneumatic pressure capsule actuated by a torque arm fastened to the casing of each motor. Thrust, or tension in the propeller shaft, is measured by a pneumatic pressure capsule, of which the piston is mounted through ball thrust bearings to the shaft and the cylinder is mounted to the housing. Both thrust and torque pressure capsules are actuated pneumatically and their operation is similar in principle to that of the meters described in reference 2. Thrust pressure is indicated as thrust force by means of a Tate-Emery load indicator, and torque pressure as torque by means of liquid manometers. The dynamometer is calibrated with the propeller shaft rotating by applying known thrusts and torques and noting the corresponding readings on the thrust scales and torque manometers. Both measurements gave straight-line calibrations.

The dynamometer housing is covered by a streamline fairing 314 inches long, including the spinners, and 36 inches in diameter at the largest section. Both propeller spinners are 26 inches in diameter and are cylindrical. The nose spinner approximates a Rankine ovoid. The shape of the spinners and forebody is such as to produce as nearly as possible uniform axial flow at the free-stream velocity in the plane of the rear propeller. The dynamometer fairing was provided with flush orifices by which the static-pressure distribution over the fairing could be measured. Pressure

orifices were also located along a radius in the spinner juncture between the fairing and the rear spinner.

A strut containing a rake of total- and static-pressure tubes was mounted from the ceiling of the wind tunnel in the propeller plane but outside the slipstream. Measurements with this rake afforded a check on the correction of the tunnel datum velocity to the equivalent free airspeed.

Propellers

All tests were made with three-blade duralumin Curtiss 89301-15 propellers, which were 10 feet in diameter. Two sets of three blades, nominally identical except for the icing condition, were used. The blades of one set were in a normally clean and serviceable condition (fig. 3) and the blades of the other set were plastered with an irregular coat of cement and burlap that simulated in outline and thickness a deposit of glaze ice that might be formed on the blades in flight (fig. 4). Figure 5 is a sketch showing principle dimensions of the ice build-up on the blades. The break in the deposit along the leading edge of the blades near the shank simulates a section of ice release. The blades bore the following identification:

Inst.	3-25-44	
Drawing	89301-15	
Angle-at-42		
Serial number	CF2J4708	(Clean blades)
Serial number	CF2J4709	
Serial number	68467	
Serial number	CF2J4703	(Simulated icing)
Serial number	CF2K5165	
Serial number	61655	

The principal physical dimensions of the Curtiss 89301-15 design blades are given in figure 6. This design uses propeller Clark Y sections and has an activity factor of 98.0 per blade.

TESTS

Tests were made at blade angles of 20°, 25°, 30°, 35°, and 40° at the 42-inch radius (0.70R) with the propeller mounted on the rear spinner of the dynamometer. Blade angles at the 45-inch radius (0.75R) are less by 1.4°. The first tests were made with the set of clean blades, and a comparison was then obtained from tests of the blades with the simulated icing. In order to make the comparison conclusive, the simulated-ice deposit was removed, the blades were thoroughly cleaned, and the tests were repeated.

A rotational speed of 1800 rpm was used for all tests to shorten and simplify the work. A range of advance ratio J was covered for each blade angle by changing the tunnel airspeed which was varied from about 120 to 420 miles per hour. At the higher blade angles, low values of advance ratio could not be obtained because of excessive power absorption at the rotational speeds at which the tests were run. A wider range of advance ratio would have been possible had additional tests been made at lower rotational speeds. Such tests were not run for two reasons: first, a mechanical difficulty, which could be eliminated by a redesign of dynamometer bearings, made it necessary to operate at moderately high speed; and second, the resultant tip speed obtained by testing at 1800 rpm simulated actual flight conditions, and the variation of air-stream Mach number with advance ratio was representative of full-scale constant-speed propeller operation.

REDUCTION OF DATA

The test results corrected for tunnel-wall interference and spinner force are presented in the form of the usual thrust and power coefficients and propeller efficiency.

Definition of propeller thrust.- Propeller thrust, as used herein, is defined as the increase in shaft tension caused by the spinner-to-tip portion of the blades rotating in the air stream. Thrust forces on the spinners due to the surrounding pressure field have been deducted from the thrust scale readings to determine propeller thrust. The spinner forces were found

by measuring thrust on the spinners operating without propeller blades at the same values of rotational speed and airspeed as were used in the tests with the propellers. A further correction was made for the fictitious thrust due to the influence of the pressure field of the propeller acting at the juncture between the spinner and the fairing. Propeller thrust then is

$$T = T_i - T_s - \Delta T_s$$

where

T_i thrust of the propeller and spinners indicated by the scales when the propeller is operating

T_s thrust on the spinners (without propeller blades) at the rotational speed and airspeed at which T_i is measured

ΔT_s change in spinner thrust due to a change in pressure at the spinner-fairing juncture

The change in spinner thrust ΔT_s varied with propeller operating conditions and was determined from pressure measurements in the juncture between the rear spinner and the fairing at the rear of the propeller. Values of thrust coefficient were changed by no more than 0.002 by this correction to the spinner thrust. The thrust on the spinner without propeller blades T_s varied with tunnel airspeed and was measured by the thrust scales while the spinner was rotating at the chosen test speed of 1800 rpm. The value of T_s varied from -7 pounds at zero dynamic pressure to 37 pounds at a dynamic pressure of 500 pounds per square foot.

Correction for wind-tunnel wall interference.- When a propeller operates in an air stream constrained by wind-tunnel walls, the velocity indicated by the wind-tunnel calibrated orifices is greater than the velocity in free air at which the propeller would produce the same thrust and torque with the same rotational speed as that used in the wind tunnel. Glauert (reference 3) has made an analysis in which he shows the velocity correction to be a function of the ratio of propeller thrust to dynamic pressure, or the ratio of thrust coefficient to

nominal advance ratio. A plot of Glauert's velocity correction for a 10-foot-diameter propeller operating in a 16-foot-diameter closed-jet tunnel is shown in figure 7. For most of the data the correction amounted to less than 2 percent.

During the tests the equivalent free airspeed was determined experimentally for a number of test points by measurements with the survey rake in the plane of the propeller outside the slipstream. The accuracy of the experimental method has been confirmed by a series of tests described in reference 4. The experimentally determined equivalent free airspeed in the present tests agreed well with the values calculated from Glauert's equation; hence only the theoretical correction has been used for all of the data.

Presentation of data.- The data are presented as plots showing the variations of thrust and power coefficients with advance ratio for the normally clean propeller in figures 8 and 9 and for the propeller with simulated icing in figures 10 and 11. The variation of test air-stream Mach number with advance ratio is also shown in these figures.

Accuracy.- The results obtained from several tests of the blades after the simulated ice was removed agreed with those obtained from tests of the original clean blades within 1 percent. The comparative data, therefore, are presented as accurate to within 1 percent.

RESULTS AND DISCUSSION

Effect of icing.- The effect of the icing condition on propeller thrust is shown in figure 12, which is a composite of the faired values of thrust coefficients for the two sets of blades tested. The simulated ice accumulation caused a loss of thrust for all blade angles throughout the J range of the tests. Figure 13 is a composite of the faired values of power coefficients for the two sets of blades, and figure 14 shows the corresponding values of efficiency plotted against advance ratio. A comparison of the envelope efficiency curves shown in figure 15 indicates that the simulated ice on the three-blade Curtiss 8930I-15 propeller caused a

decrease in peak efficiency of 2.5 to 3.0 percent over the range of advance ratio of the tests. This decrease in efficiency is a result of the loss of blade section lift and the increase of blade section drag as shown by the J values at zero thrust and power.

Constant-power propeller operation.- Inasmuch as an airplane often operates over a large range of advance ratio at constant rotational speed and torque (constant-power coefficient at constant air density), the data were analyzed at two representative values of constant-power coefficient. The results of this analysis, presented in figure 16, indicate that the efficiency loss due to a mild icing condition is relatively small except under unrepresentative operating conditions in which the propeller is very lightly loaded (as in a shallow dive).

APPLICATION OF ICED-WING AIRFOIL CHARACTERISTICS TO PROPELLER ANALYSIS

The purpose in making this propeller analysis based on airfoil data was twofold: first, to find out whether the calculated decrease in propeller efficiency was of the same magnitude as that found experimentally and, second, to obtain an indication of the effect of premature stalling of the iced blades. The simplified method used for calculating propeller characteristics from airfoil data is that given by Lock in reference 5. The airfoil data used were those obtained from full-scale-tunnel tests of an NACA 0012 airfoil of aspect ratio 6 with and without a simulated ice deposit (reference 1). These airfoil data reduced to infinite aspect ratio for use with Lock's method are presented in figure 17. The propeller characteristics calculated by the simplified method with airfoil data are not presented for use as propeller data but merely to show the changes that may be expected when propeller blades become fouled by a mild ice deposit.

In applying the airfoil data to the propeller analysis, a tacit assumption was made that the propeller blades were iced uniformly from hub to tip in a manner similar to the icing on the wing. In the propeller tests, the blades were not uniformly iced but a large portion of the tips was left clean. Because the

icing simulated on the wing was composed of small rough mounds, it was probably more detrimental to the section lift and drag than were the continuous glazed patches cemented to the propeller blades. For both of these reasons the calculations would be expected to show a greater loss than the propeller tests. Although the general agreement was good, the calculations did actually show a greater loss than did the tests.

The calculated propeller characteristics for a blade angle of 30° are presented in figure 18 for both the normally clean and the iced condition. The values of thrust coefficient indicate a probable serious loss of thrust at the lower values of advance ratio when the blades become iced. In order to maintain flight at the maximum thrust coefficient with the blades not stalled, the iced propeller must be operated at a value of advance ratio at least 0.3 greater than is required for the clean propeller. If a propeller has been selected to operate normally under rather high load for a given flight condition, it might easily be forced to operate partly stalled for the same condition if it should become fouled with ice. This argument might apply especially when ice formation, by increasing the weight of an airplane and decreasing its aerodynamic efficiency, forces the airplane to attempt to climb at relatively low speed. For example, a propeller operating normally at a value of advance ratio of 0.55 and a thrust coefficient of 0.156 would lose about 15 percent efficiency when iced.

The results of further computations of only peak efficiency for a series of different blade angles over a wide range of advance ratio are presented in figure 19. These computations indicate a loss of approximately 5 percent in peak efficiency for the iced propeller over the range of advance ratio considered.

CONCLUSIONS

High-speed wind-tunnel tests of a full-scale three-blade Curtiss 89301-15 propeller with and without a deposit of simulated ice on the blades led to the following conclusions:

1. The simulated icing condition caused a decrease in peak efficiency of 2.5 to 3.0 percent over a range of advance ratio of 0.7 to 1.8.

2. Computations of propeller performance based on airfoil data for an icing condition comparable with that of the propeller tested indicated peak efficiency losses of about the same magnitude as the measured losses.

3. The calculations also indicated that a propeller chosen for high cruising efficiency but for operation at large values of thrust coefficient in climb might become stalled in climb as a result of icing, with a possible attendant loss of efficiency of about 15 percent.

Langley Memorial Aeronautical Laboratory
National Advisory Committee for Aeronautics
Langley Field, Va., April 2, 1946

REFERENCES

1. Gulick, Beverly G.: Effects of a Simulated Ice Formation on the Aerodynamic Characteristics of an Airfoil. NACA ACR, May 1938.

2. Moore, Charles S., Biermann, Arnold E., and Voss, Fred: The NACA Balanced-Diaphragm Dynamometer-Torque Indicator. NACA RB No. 4C28, 1944.

3. Glauert, H.: The Elements of Aerofoil and Airscrew Theory. American ed., The Macmillian Co., 1943, pp. 222-226.

4. Lock, C. N. H., and Bateman, H.: The Effect of Wind Tunnel Interference on a Combination of Airscrew and Tractor Body. R. & M. No. 919, British A.R.C. 1924.

5. Lock, C. N. H.: A Graphical Method of Calculating the Performance of an Airscrew. R. & M. No. 1849, British A.R.C., 1938.

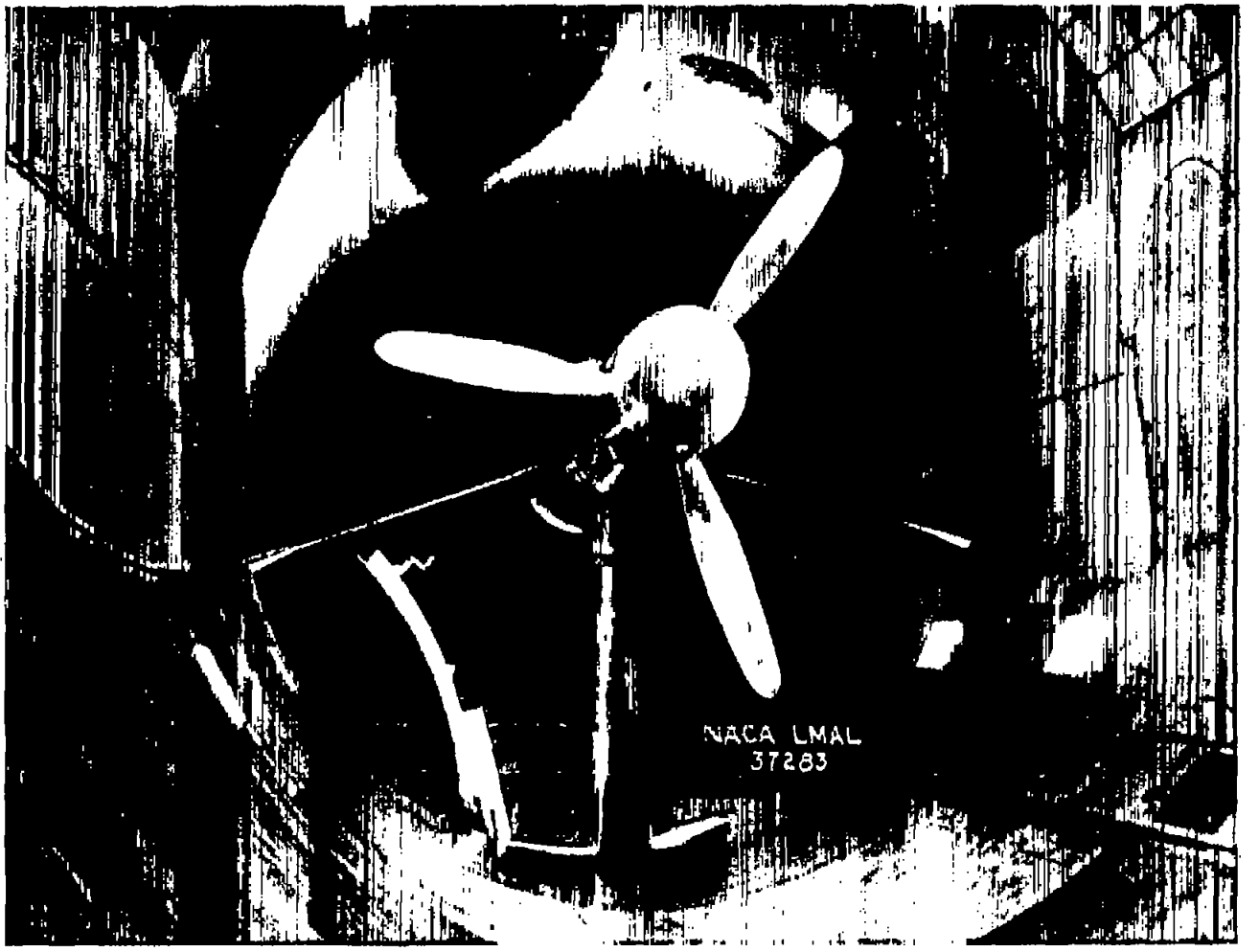

Figure 1.- Propeller dynamometer in test section. Clean blades.

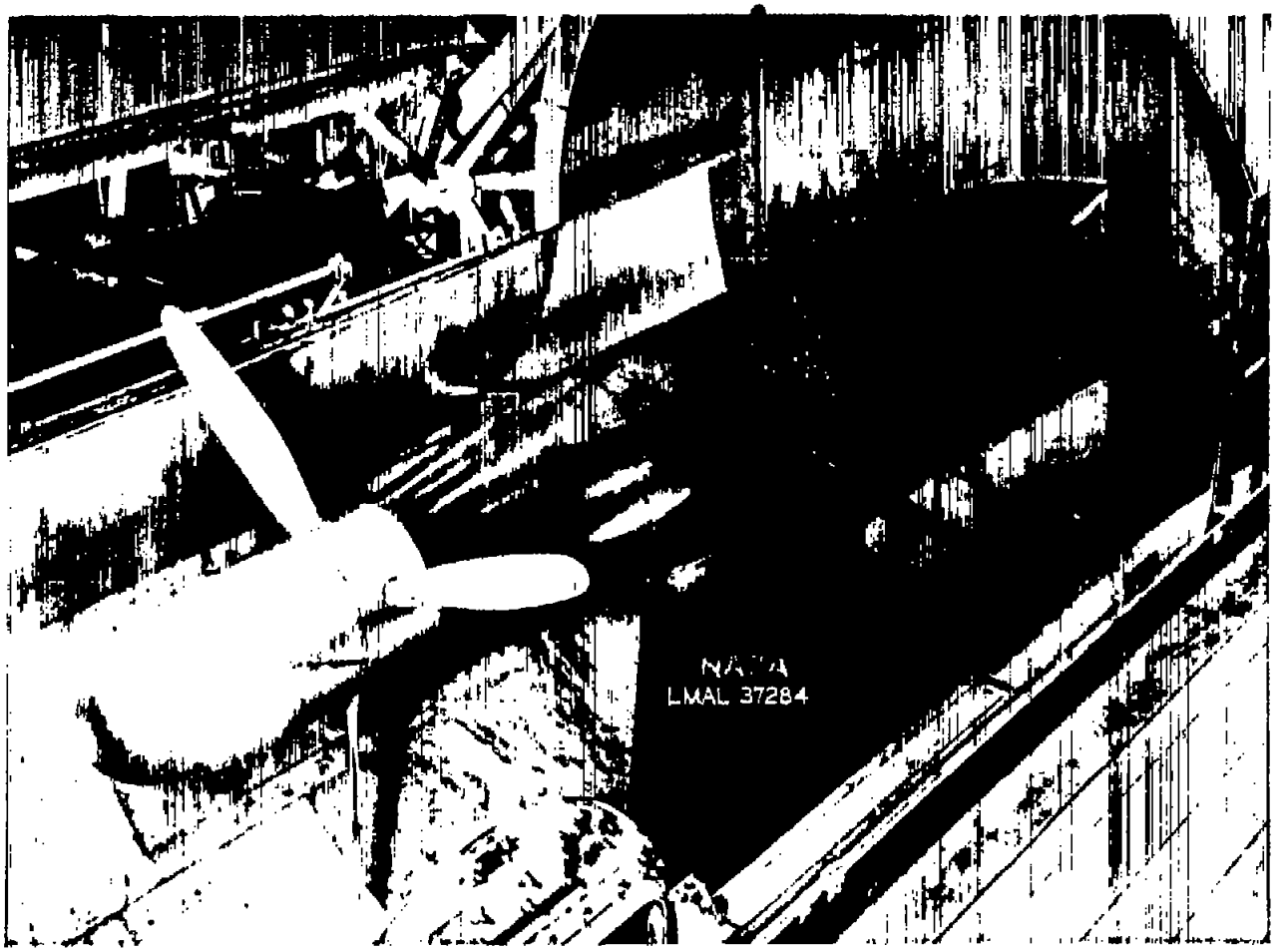

Figure 2.- Propeller dynamometer in test section. Clean blades; tunnel open.

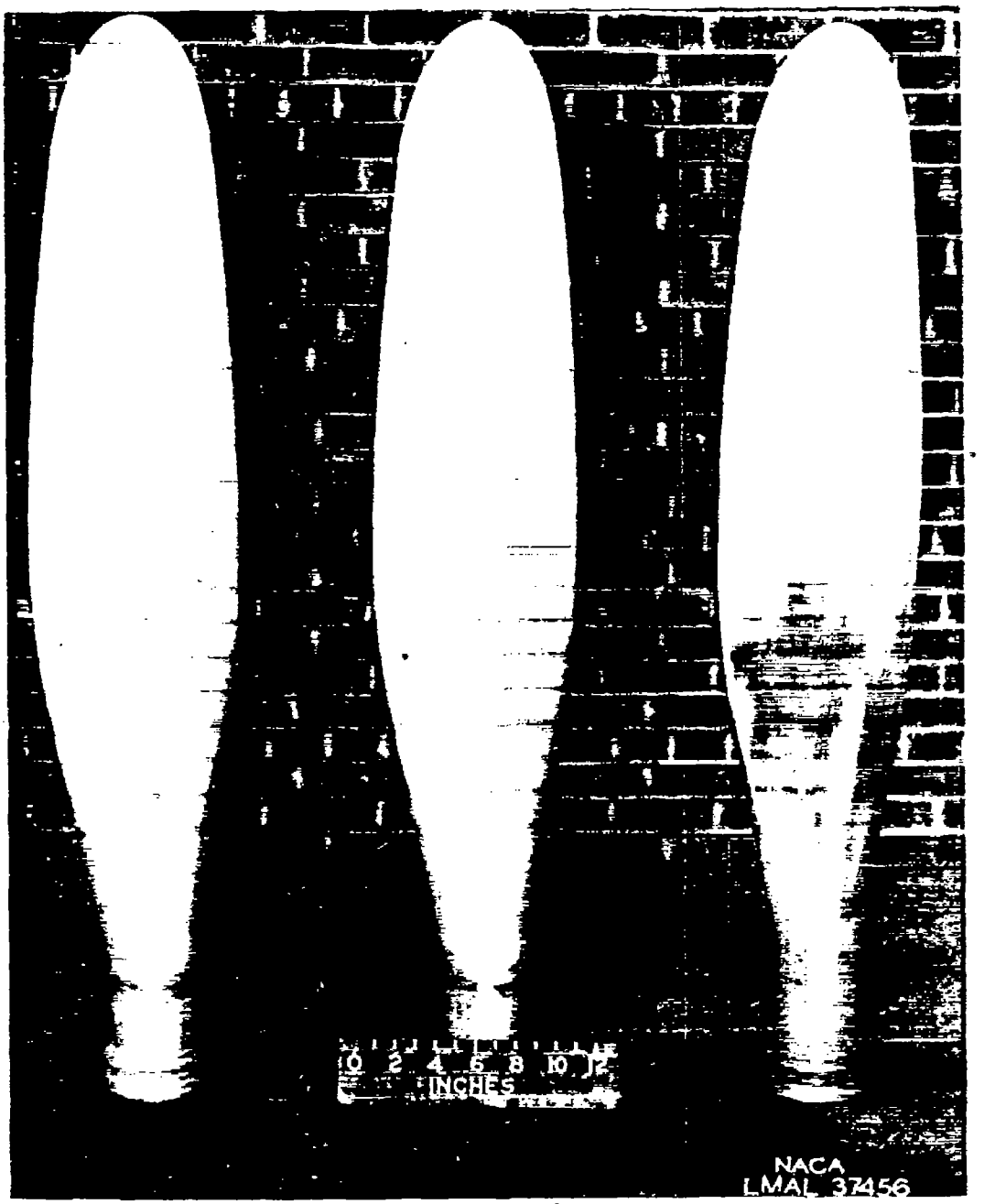

(a) Thrust face (lower surface).

Figure 3.- Curtiss 89301-15 propeller blades without simulated icing.

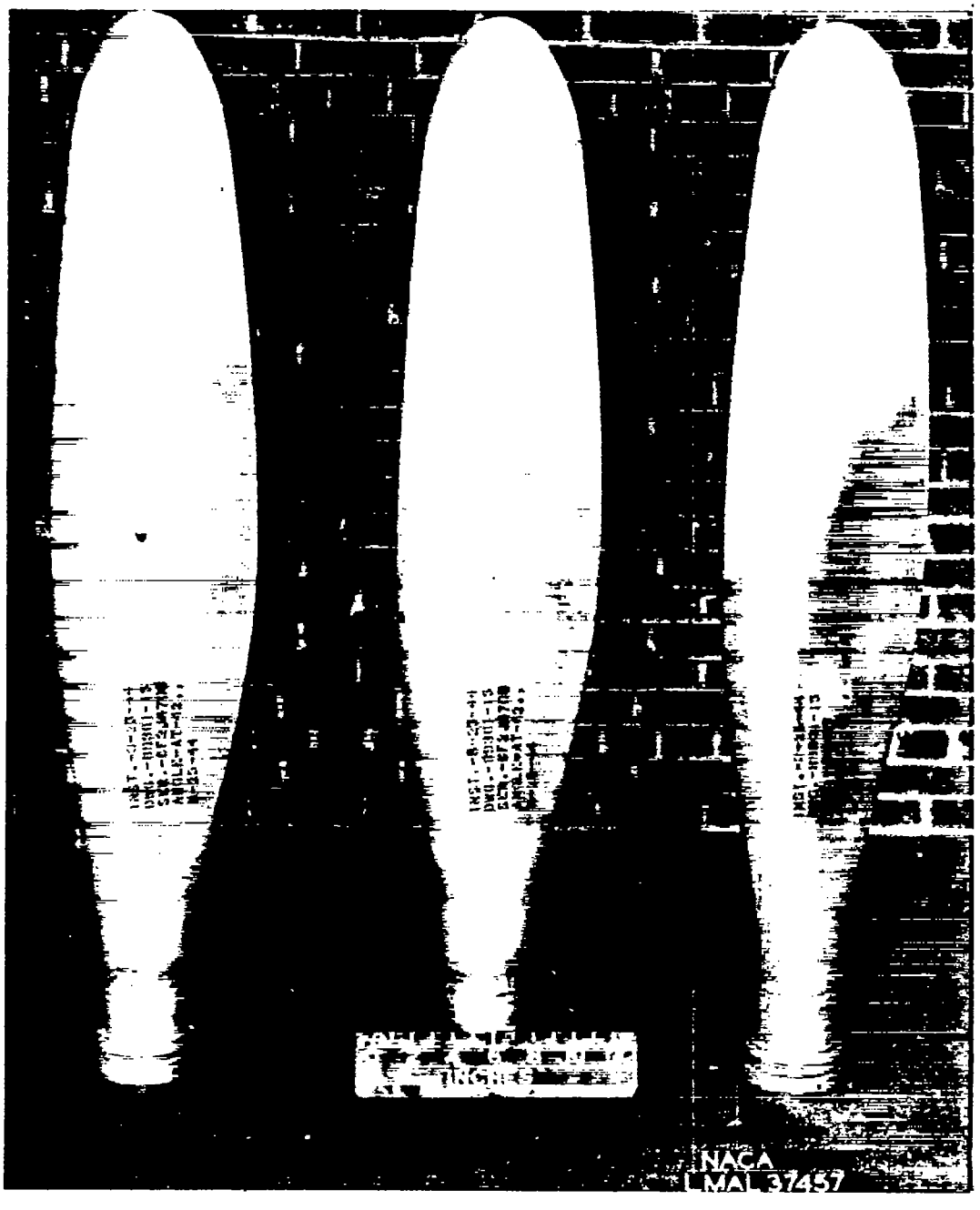

(b) Cambered face (upper surface).

Figure 3.- Concluded.

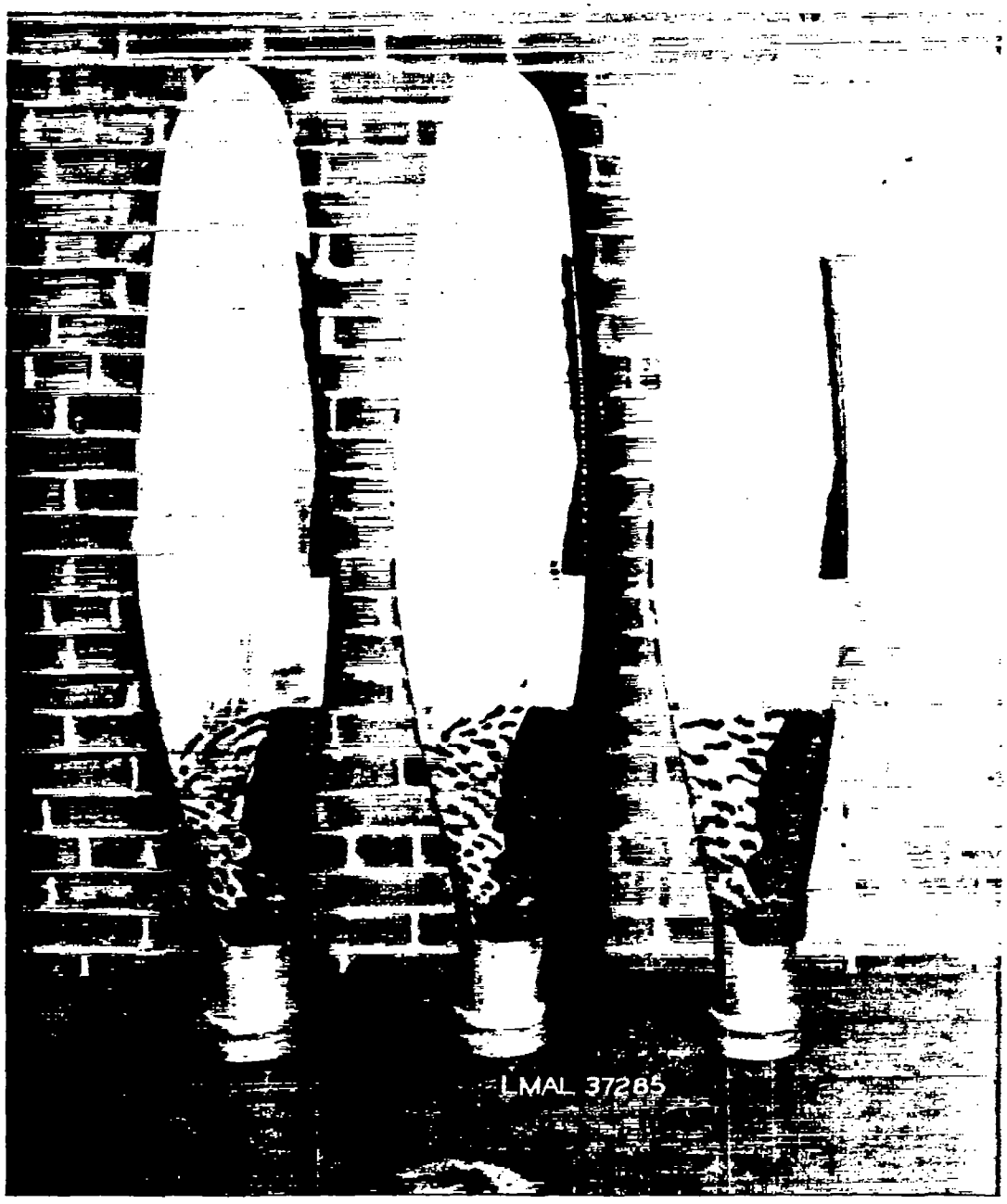

(a) Thrust face (lower surface).

Figure 4.- Simulated icing on Curtiss 89301-15 propeller blades.

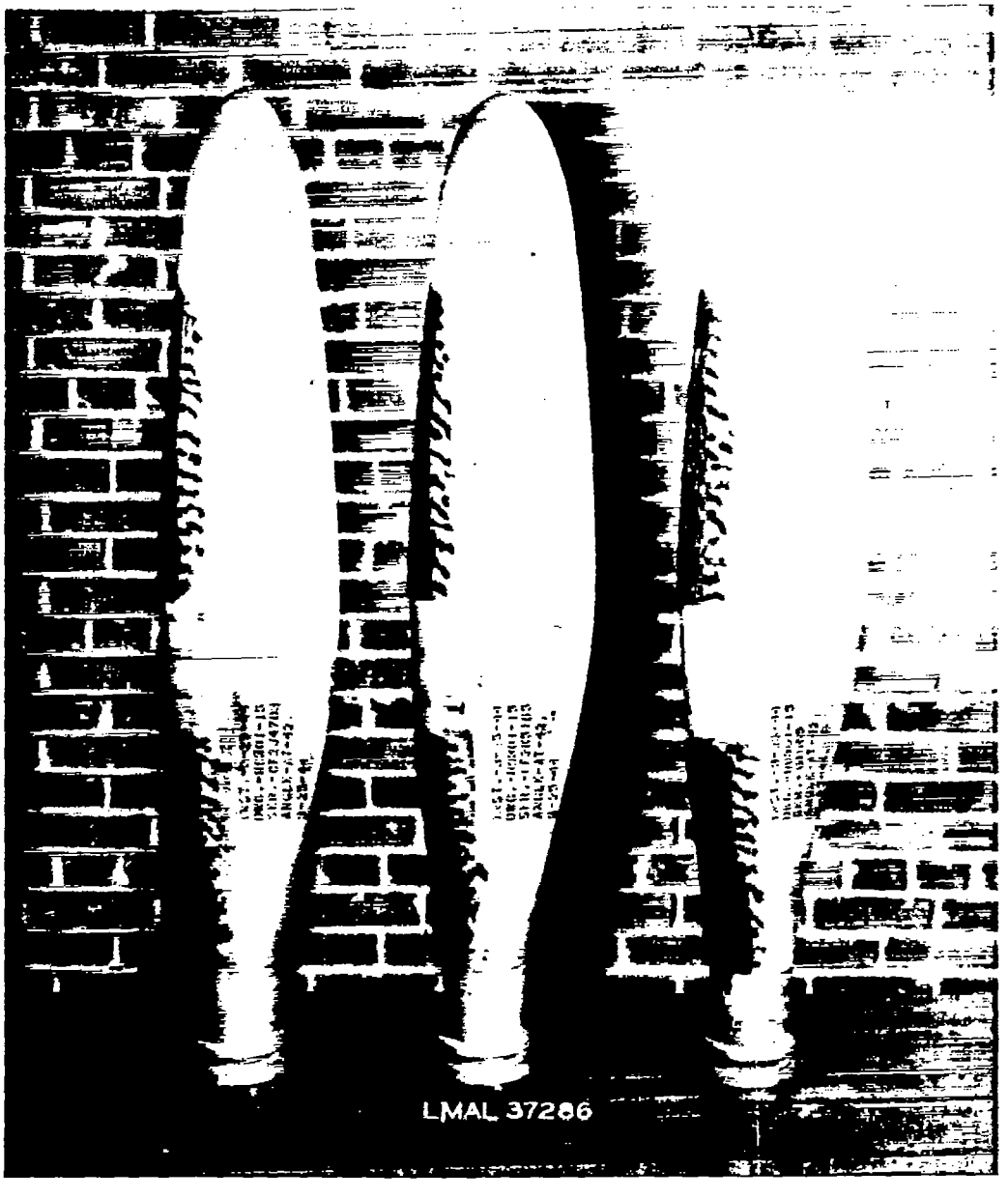

(b) Cambered face (upper surface).

Figure 4.- Concluded.

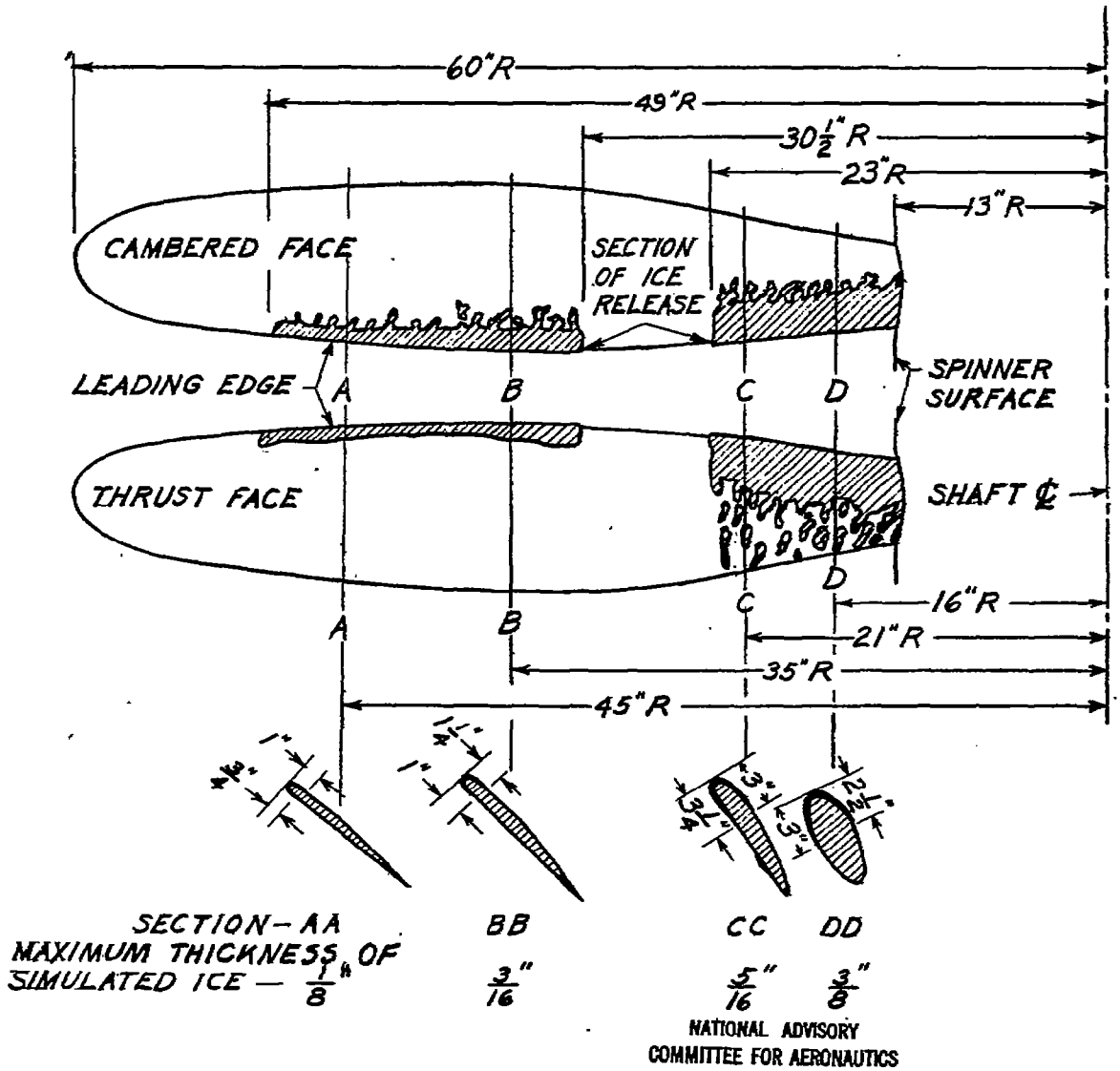

FIGURE 5.- APPROXIMATE DIMENSIONS OF THE ICE BUILD-UP ON CURTISS 89301-15 PROPELLER BLADES.

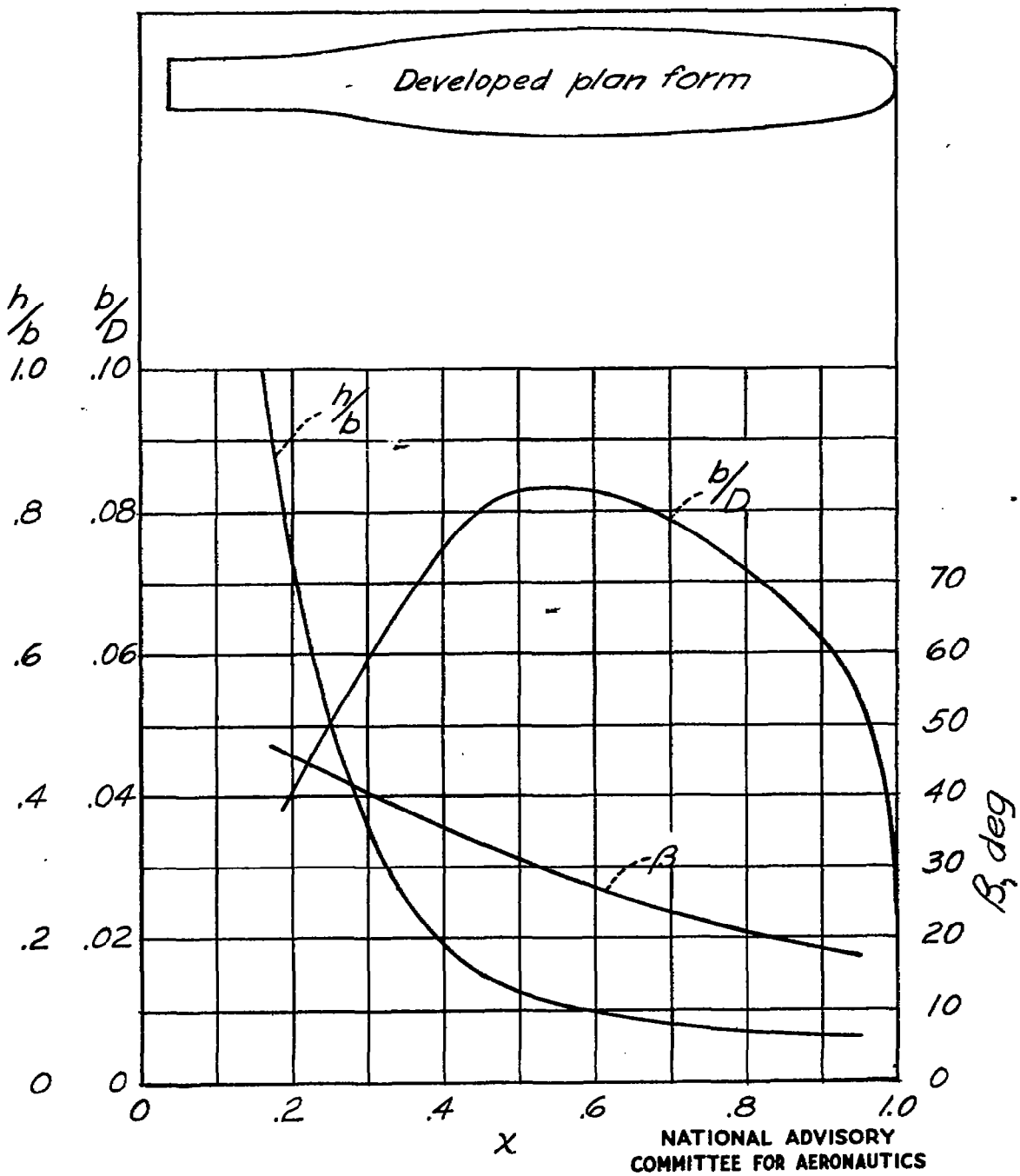

Figure 6.- Blade-form curves for Curtiss 89301-15 propeller. Activity factor, 98.0.

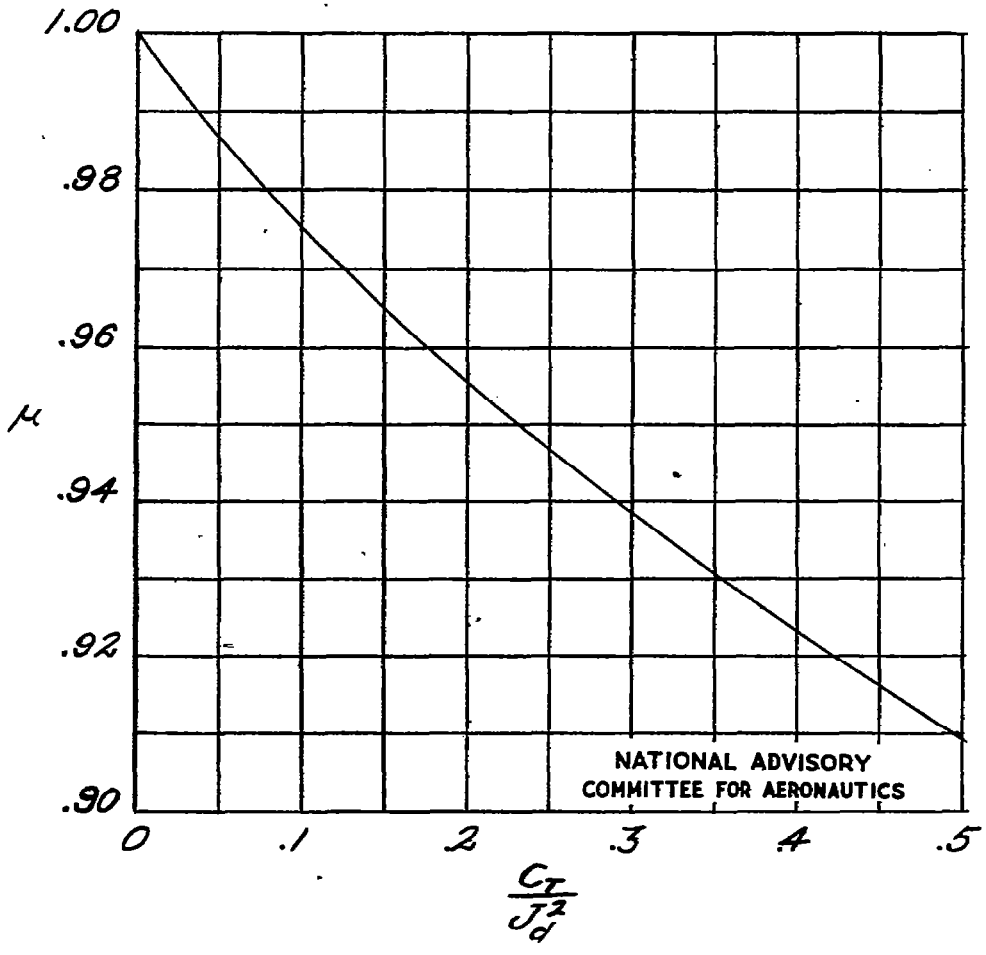

Figure 7. - Glauert's factor for correcting wind-tunnel datum velocity to equivalent free airspeed for a 10-foot-diameter propeller in a closed 16-foot circular test jet.

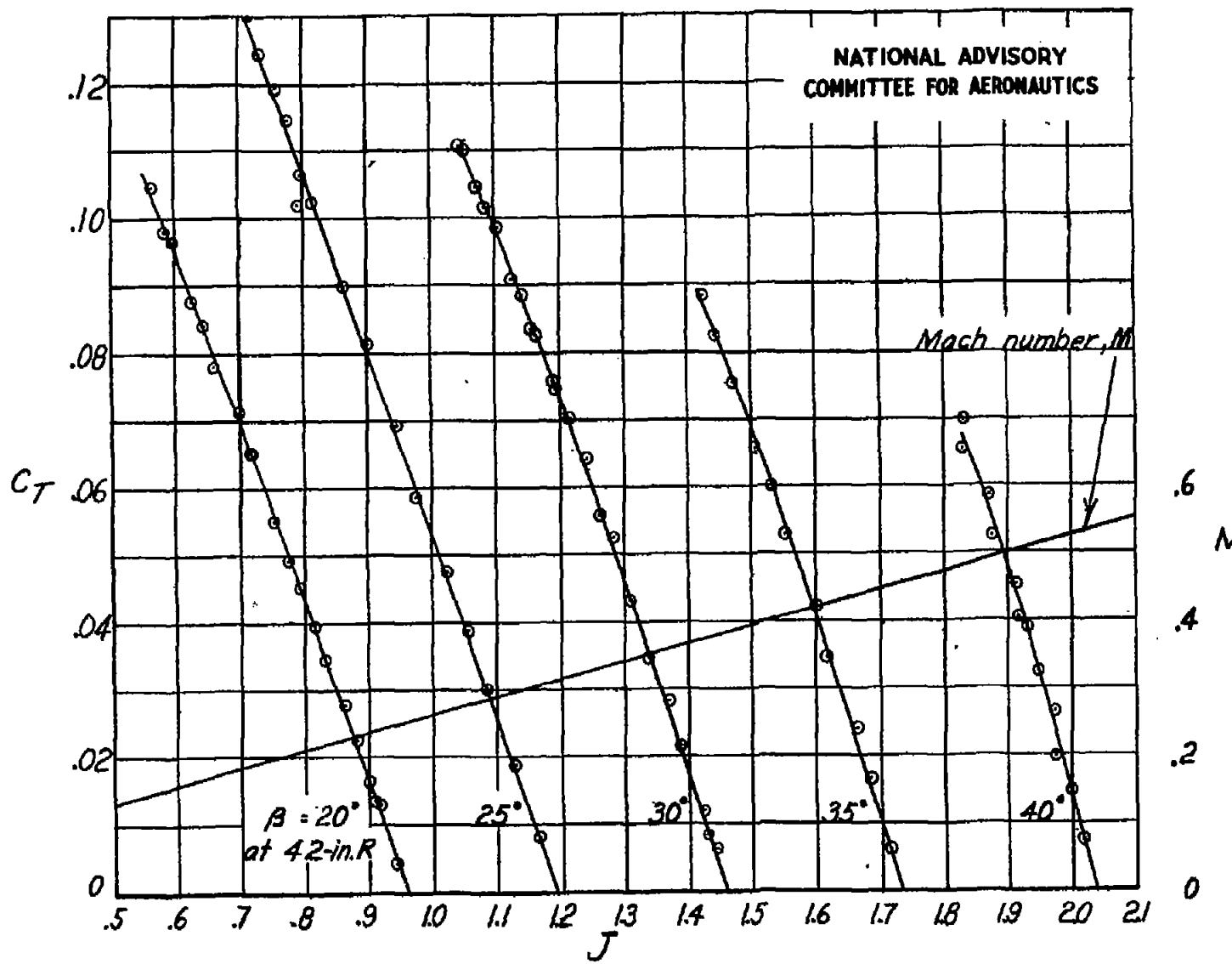

Figure 8.- Variation of thrust coefficient with advance ratio. Clean blades; D = 10 feet.

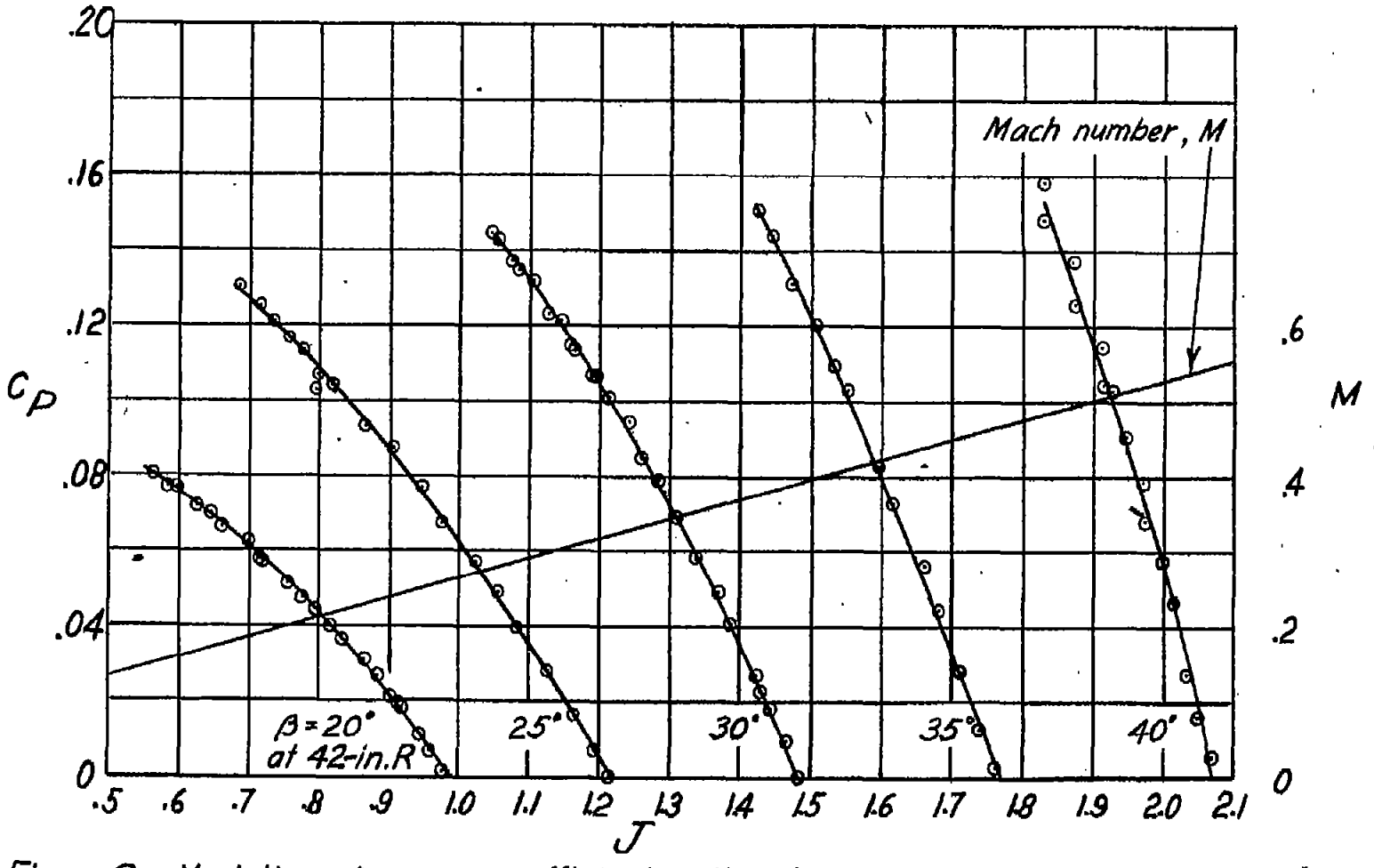

Figure 9.– Variation of power coefficient with advance ratio. Clean blades; D = 10 feet.

NATIONAL ADVISORY
COMMITTEE FOR AERONAUTICS

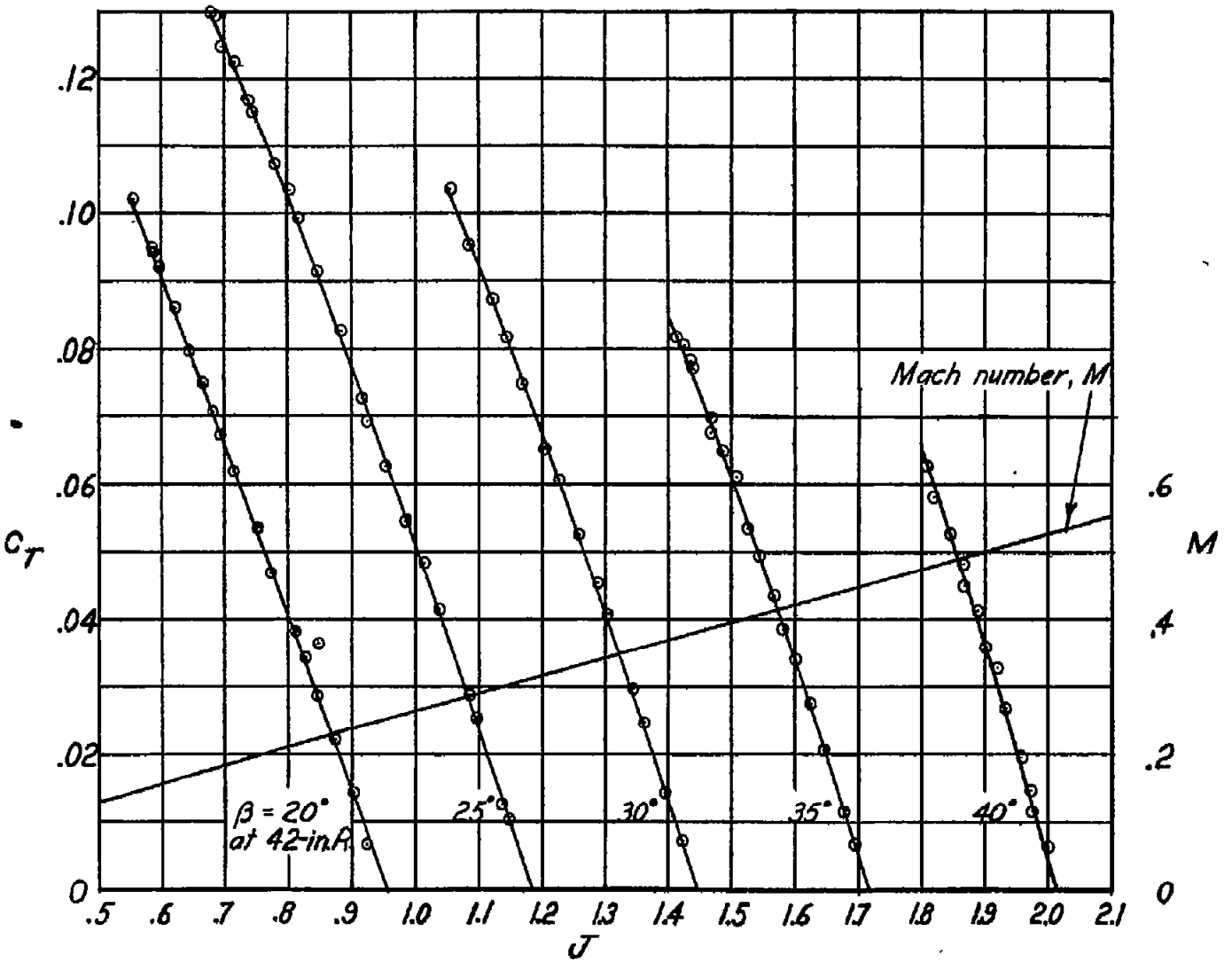

Figure 10.- Variation of thrust coefficient with advance ratio. Simulated ice on blades; D = 10 feet.

NATIONAL ADVISORY
COMMITTEE FOR AERONAUTICS

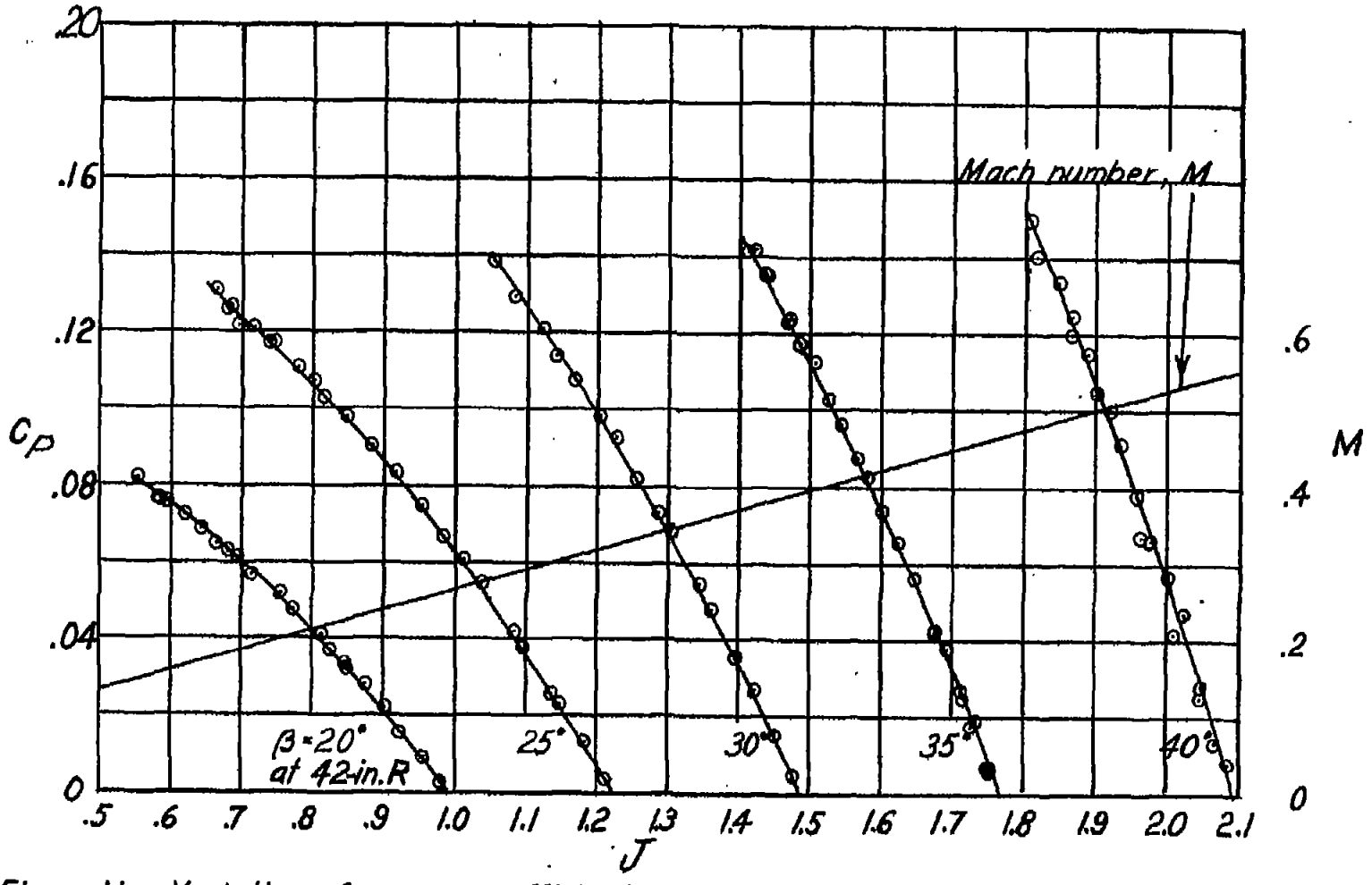

Figure 11.- Variation of power coefficient with advance ratio. Simulated ice on blades; D = 10 feet.

NATIONAL ADVISORY
COMMITTEE FOR AERONAUTICS

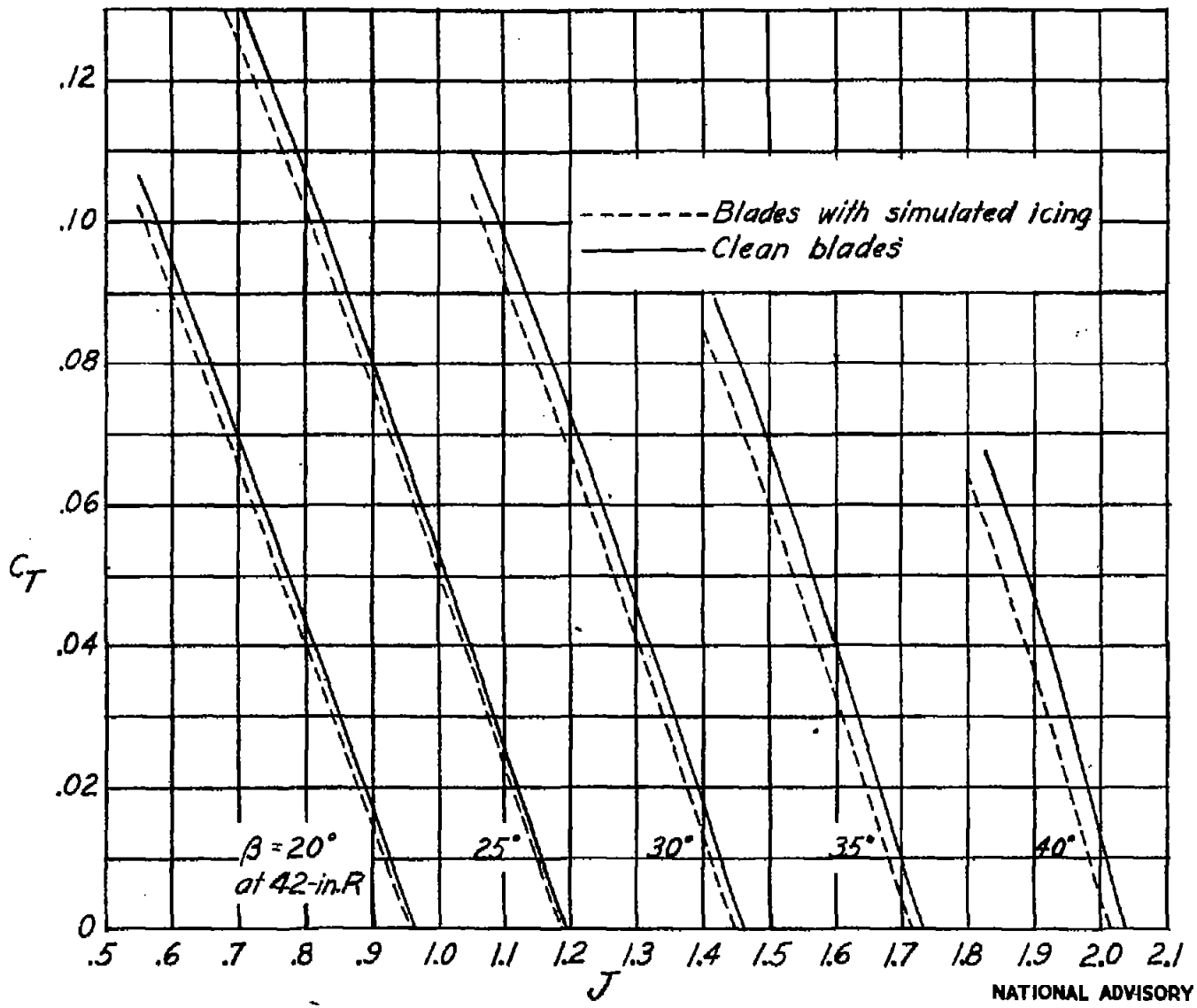

Figure 12.- The effect of icing on thrust coefficient. D = 10 feet.

NATIONAL ADVISORY
COMMITTEE FOR AERONAUTICS

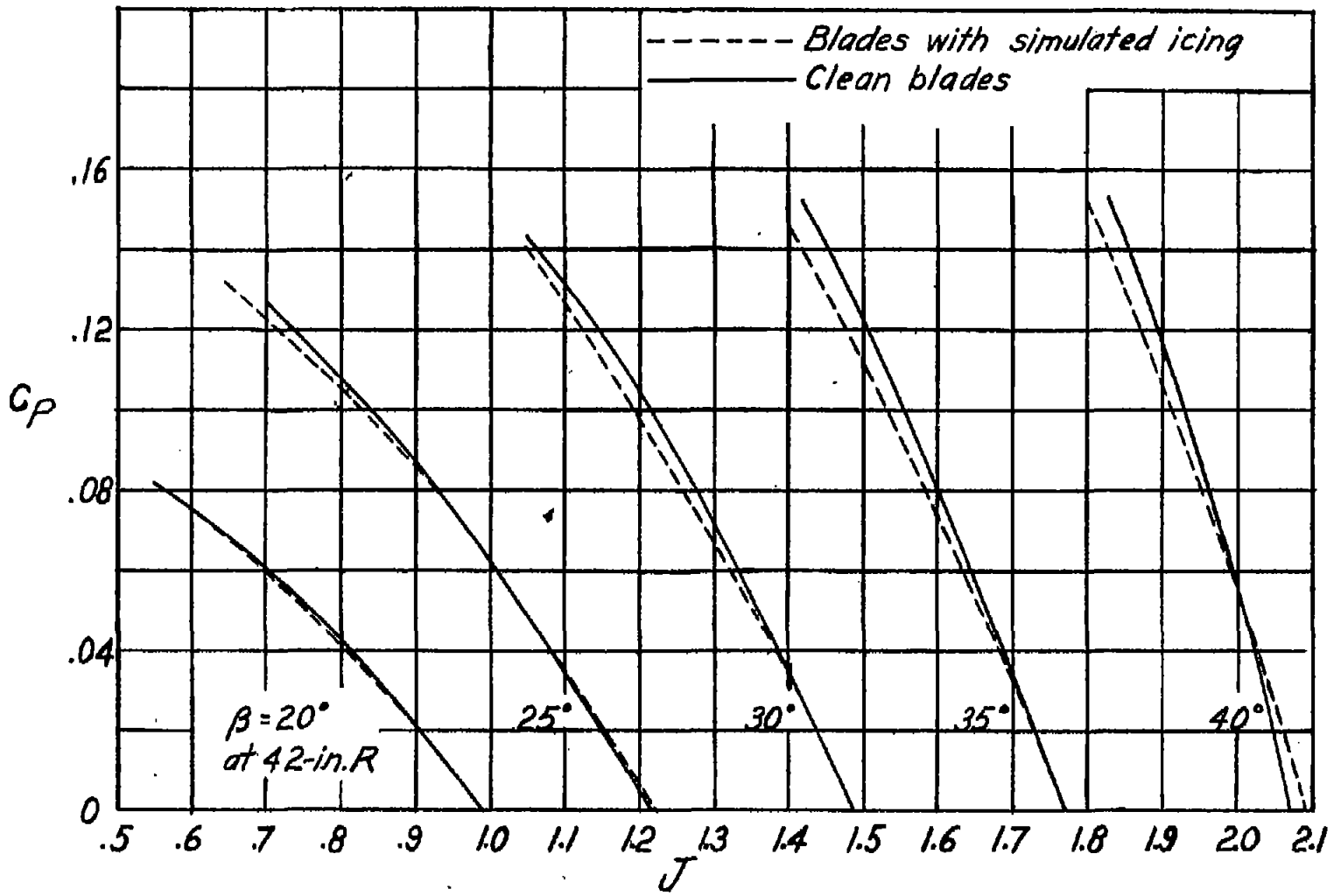

Figure 13.- The effect of icing on power coefficients. D = 10 feet.

NATIONAL ADVISORY
COMMITTEE FOR AERONAUTICS

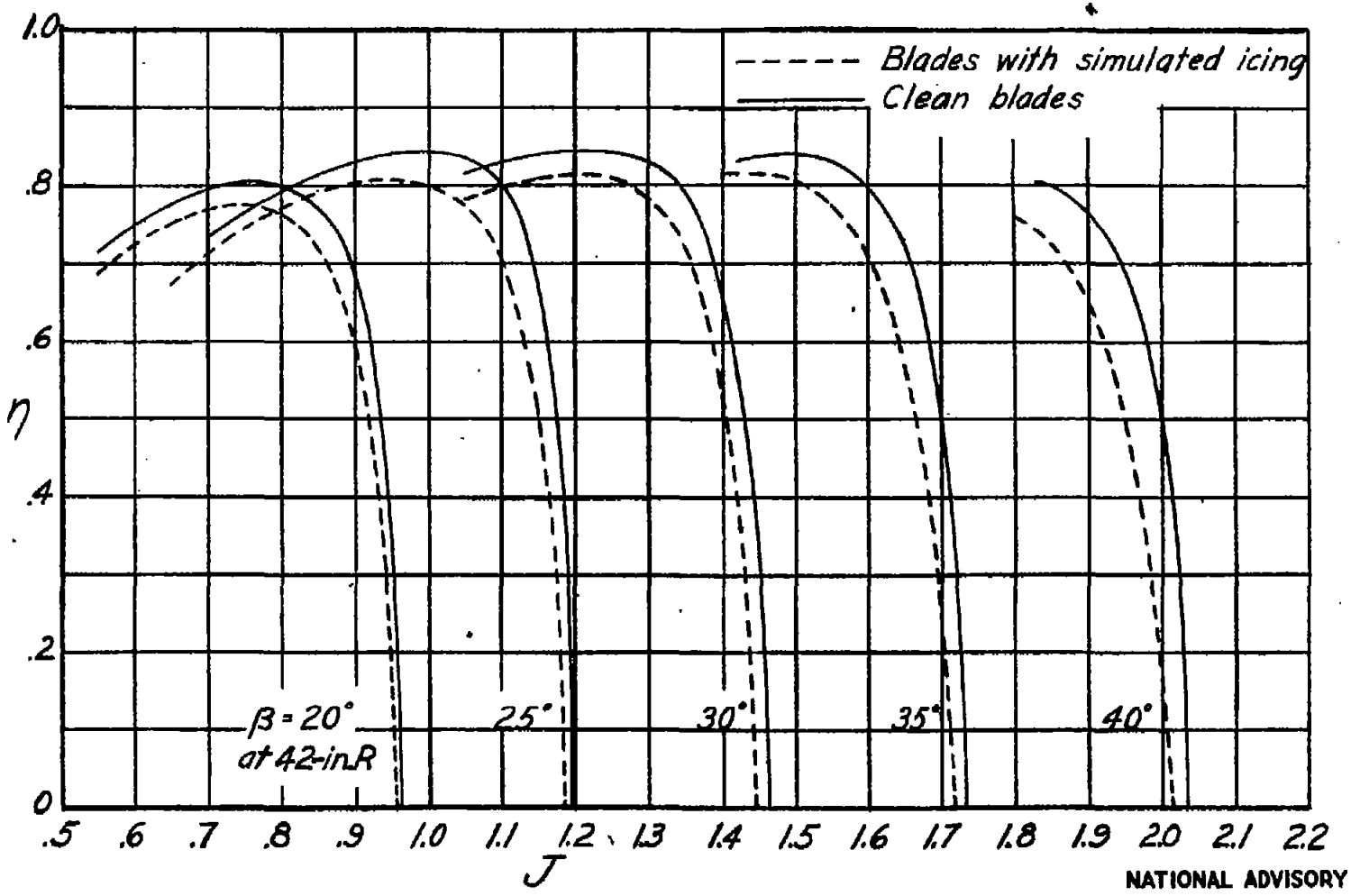

Figure 14.- The effect of icing on propeller efficiency. D = 10 feet.

NATIONAL ADVISORY COMMITTEE FOR AERONAUTICS

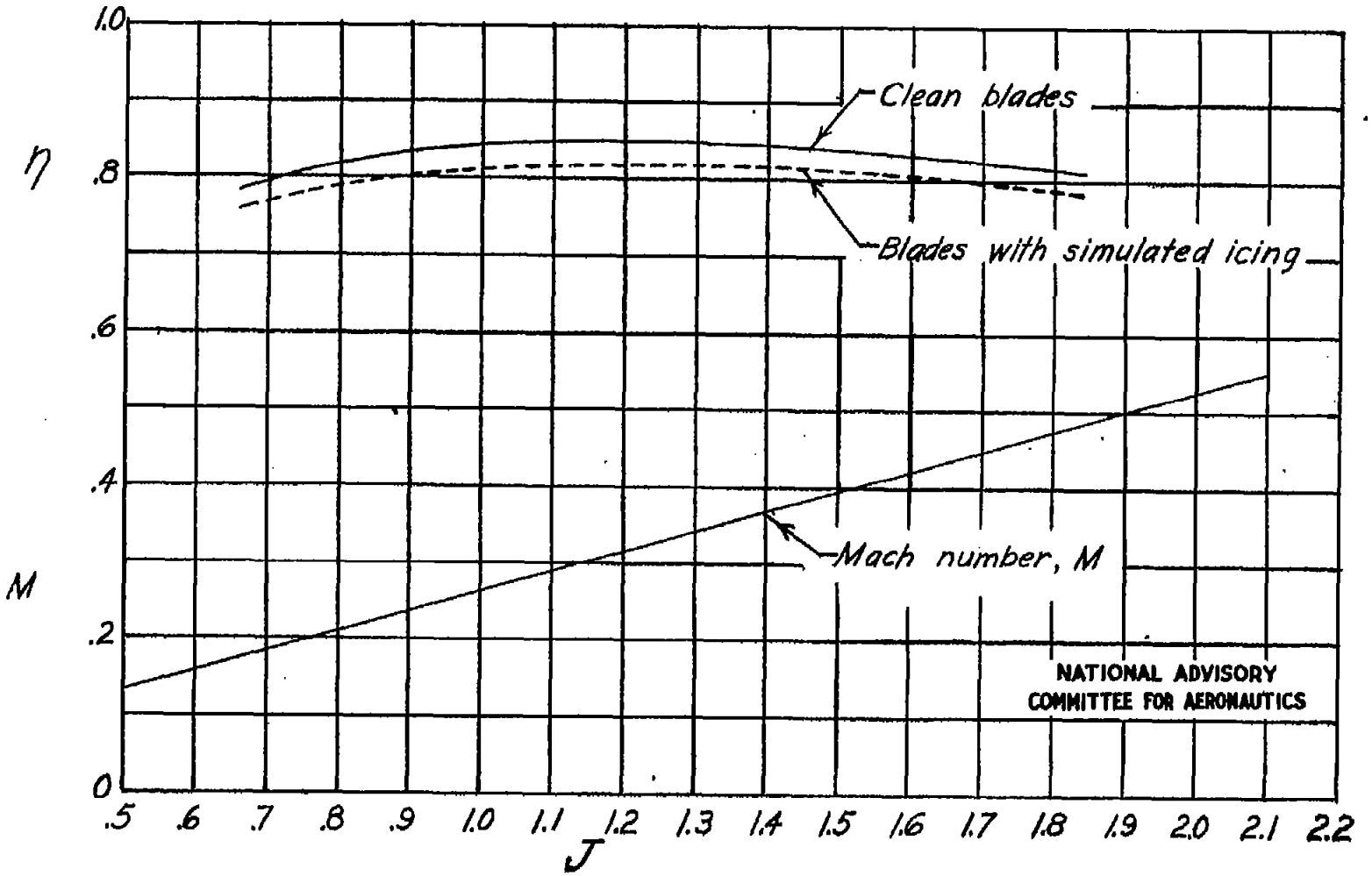

Figure 15.- A comparison of envelope propeller efficiencies to show effect of icing.

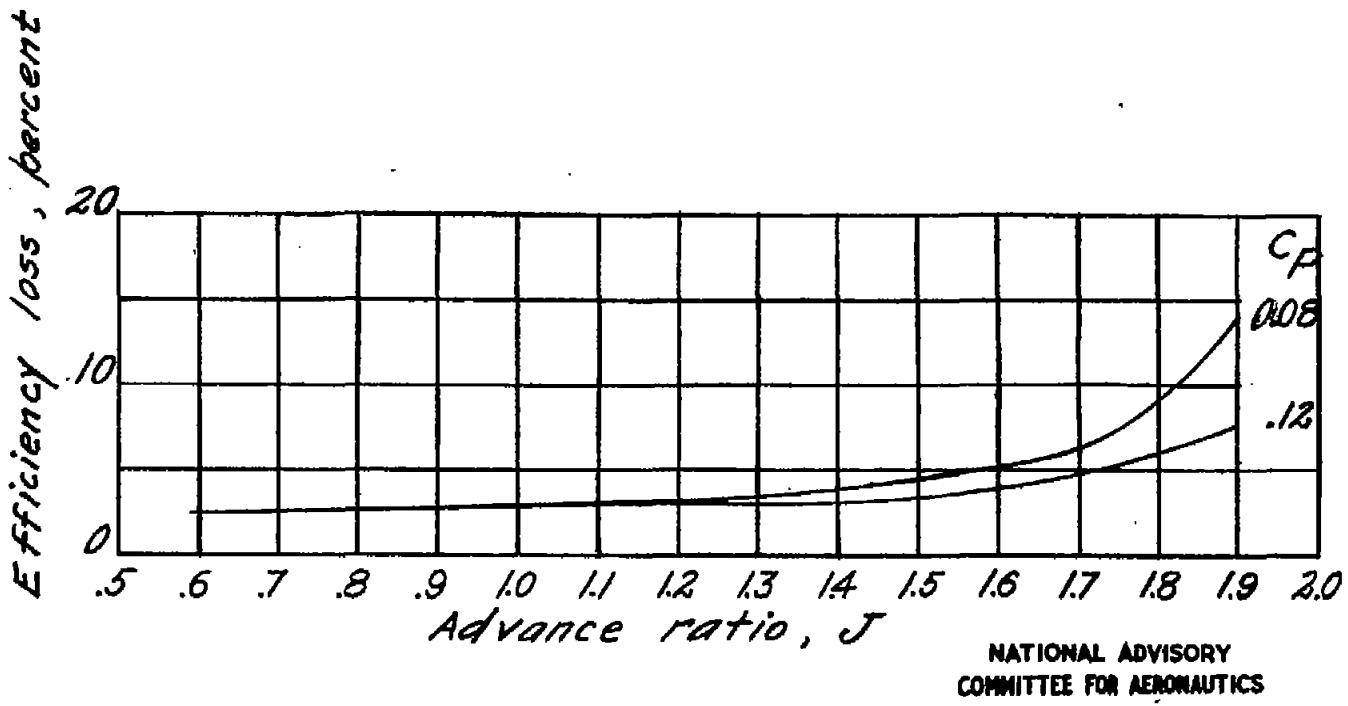

Figure 16.- Propeller efficiency loss due to ice formation for operation at constant-power coefficient.

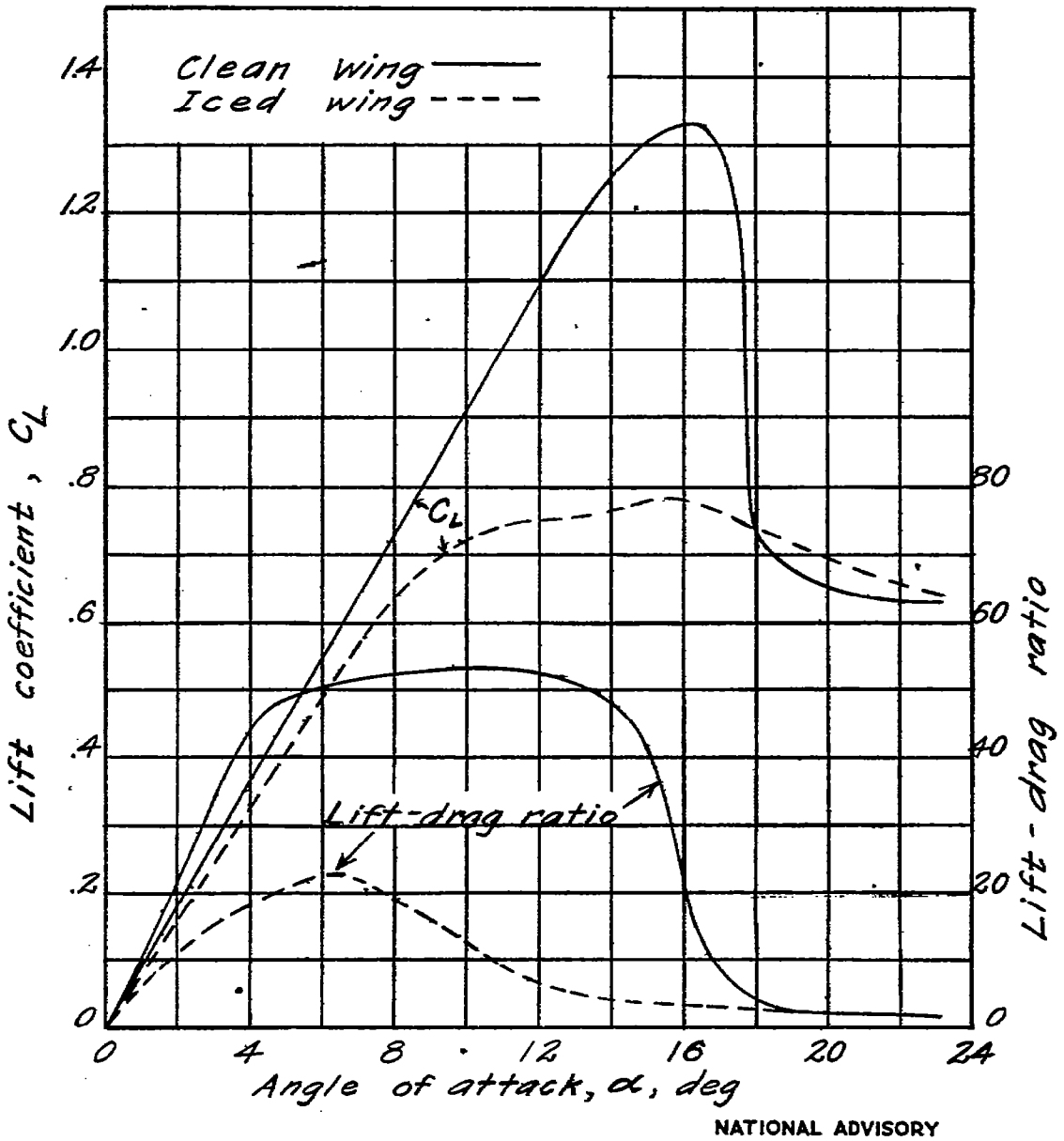

NATIONAL ADVISORY
COMMITTEE FOR AERONAUTICS

Figure 17.- Characteristics of an NACA 0012 airfoil for infinite aspect ratio.

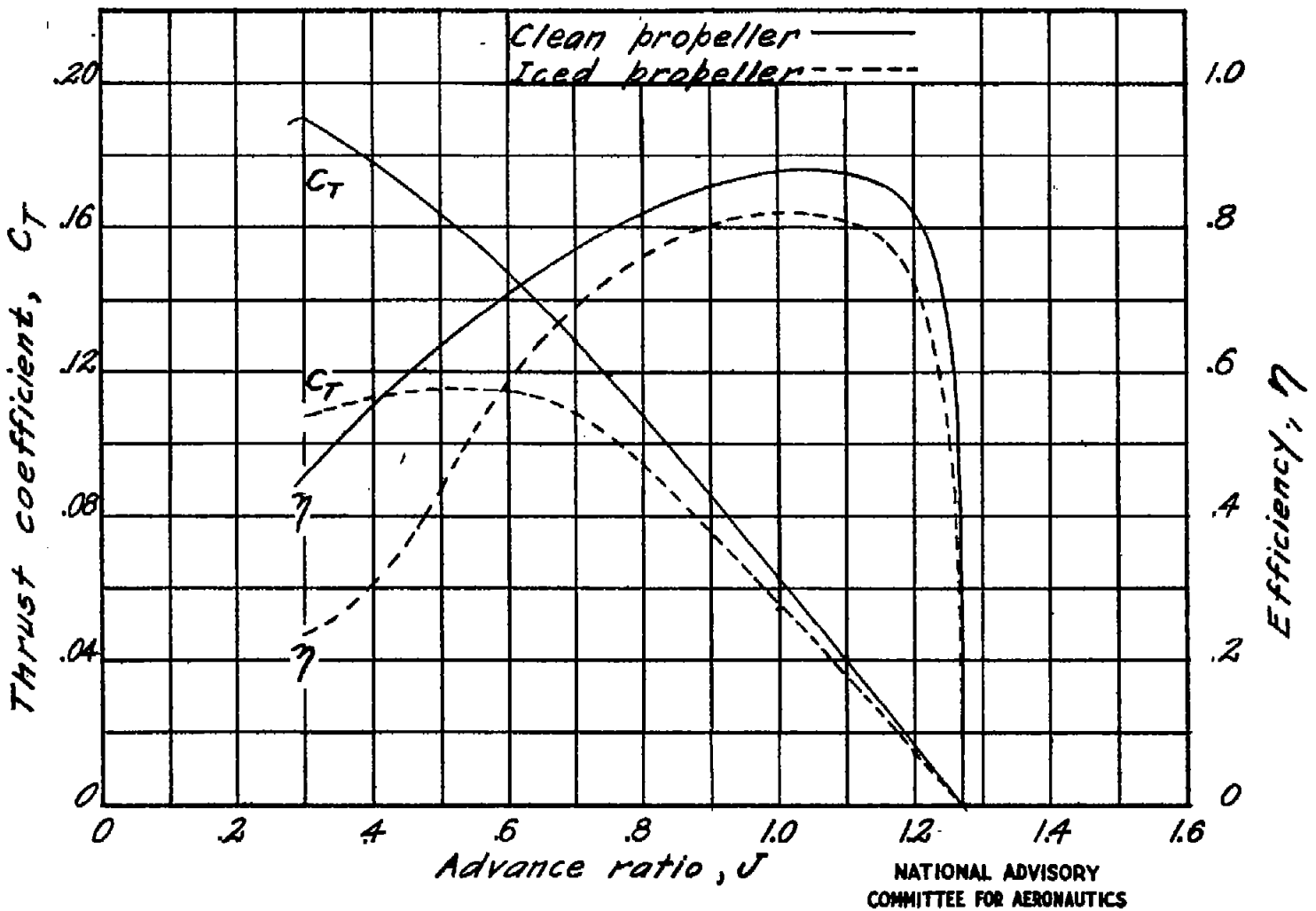

Figure 18.- Calculated propeller characteristics. NACA 0012 blade sections ; β, 30° at 42-inch R.

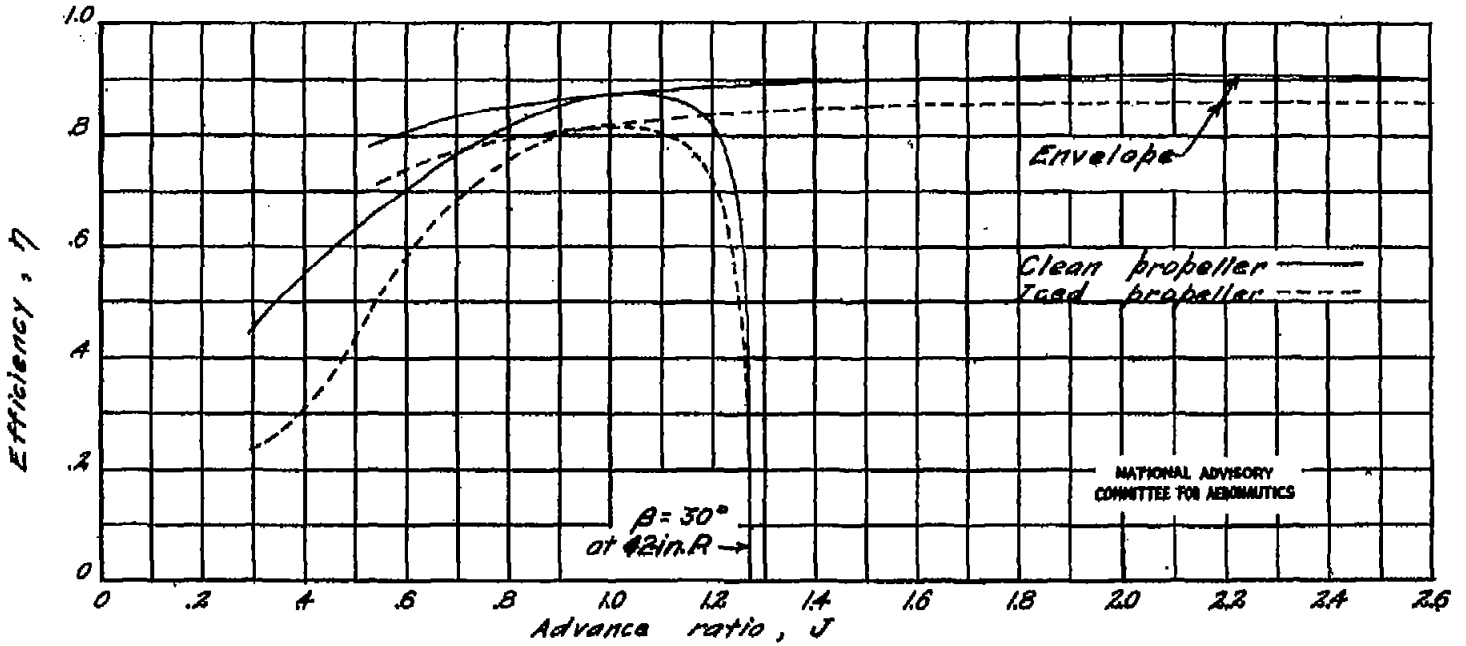

Figure 19.- Envelope curves of calculated propeller efficiency, NACA 0012 blade sections. D = 10 feet.